Optical spectrum of SN 1978K: emission from shocked clouds in the circumstellar wind

N. N. Chugai,[1,2] I. J. Danziger[2] and M. Della Valle[2,3]
[1] *Institute of Astronomy, Russian Academy of Sciences, Pyatnitskaya 48, 109017 Moscow, Russia*
[2] *European Southern Observatory, Karl-Schwarzschild St. 2, D-85748 Garching bei München, Germany*
[3] *University of Padova, Vicolo dell'Osservatorio, 5, I-35100 Padova, Italy*

ABSTRACT

An optical spectrum of SN 1978K (NGC 1313) in the range of 4000–7200 Å was obtained on 1992 October 22, i.e. 14.4 yr after the outburst. The spectrum is still dominated by the narrow (FWHM ≤ 560 km s^{-1}) Hα line having a luminosity 2.2×10^{38} erg s^{-1} ($D = 3.7$ Mpc, $A_V = 0.64$ mag), 1.5–2 times lower than the values derived from published data for 1989 December and 1990 October. There is no evidence for a broad Hα component (HWZI ~ 3000–$10\,000$ km s^{-1}) with an upper limit of luminosity $\sim 3 \times 10^{36}$ erg s^{-1}. We suggest that the optical emission of SN 1978K originates from radiative shock waves propagating in the dense ($\sim 4 \times 10^6$ cm^{-3}) clouds of a circumstellar wind. The cloud shock waves are driven by the expanding low-mass ($M \leq 2 M_\odot$) supernova ejecta with the present radius $\sim (2$–$3) \times 10^{17}$ cm. The mass of circumstellar material involved in the dynamical interaction is $\approx 1 M_\odot$ and the corresponding mass-loss rate of pre-SN wind is $\sim 2 \times 10^{-4} M_\odot$ yr^{-1}. The observed X-ray emission is attributed to the shock waves in the boundary layer of the same population of clouds. Alternatively, however, the X-ray emission might emanate from the shock waves in a different cloud population with a lower density.

Key words: shock waves – circumstellar matter – stars: mass-loss – supernovae: individual: SN 1978K.

1 INTRODUCTION

The extraordinary supernova SN 1978K in NGC 1313, discovered in 1990 January (Ryder and Dopita 1990; Ryder et al. 1993) 12 yr after the outburst, is characterized by strong narrow emission lines [750 km s^{-1} full-width zero-intensity (FWZI)] with Hα luminosity ($L > 10^{38}$ erg s^{-1}), and a powerful radio ($L_\nu(6\ \mathrm{cm}) \approx 2 \times 10^{27}$ erg cm^{-2} s^{-1} Hz^{-1}) and tremendous X-ray luminosity ($L_x \approx 10^{40}$ erg s^{-1}). It was rediscovered on three archival plates in 1978 and was classified as a type II supernova which exploded in mid-1978 (Ryder et al. 1993).

In fact, the phenomenon of SN 1978K had at least one precedent. SN 1986J, detected presumably 4 yr after the explosion, in many respects resembles SN 1978K: 7–9 years after the explosion the former shows strong Hα with FWHM 500–600 km s^{-1} and luminosity $\sim 10^{38}$ erg s^{-1} (Leibundgut et al. 1991), strong radio emission (Weiler, Panagia & Sramek 1990), $L_\nu(6\ \mathrm{cm}) \approx 10^{28}$ erg cm^{-2} s^{-1} Hz^{-1} and a powerful X-ray luminosity $L_x \sim 5 \times 10^{40}$ erg s^{-1} (Bregman & Pildis 1992). The similarity of these two supernovae was noted immediately after the discovery of SN 1978K (Filippenko 1992).

Observational data for SN 1978K obtained in radio, optical and X-ray bands have been discussed by Ryder et al. (1993). They concluded that the optical, X-ray and radio emission is the result of the interaction of the expanding supernova envelope with the dense circumstellar (CS) medium created by extreme mass loss from a massive progenitor. The overall mass of the CS material involved in the dynamical interaction with the supernova envelope was estimated to be $M > 80 M_\odot$.

The assumption of an extremely large mass of CS material in the close vicinity of massive stars (~ 0.1 pc) is not, however, easy to reconcile with the standard picture of the stellar evolution of massive stars. Therefore any alternatives alleviating the problem of such a large mass of CS material are welcome. Earlier the optical and X-ray emission of SN 1986J, the close counterpart of SN 1978K, have been interpreted with the model of the interaction of the supernova envelope with a clumpy wind (Chugai 1993). It was conjectured also that the same mechanism is operating in SN 1978K.

Here we present new spectrophotometry of SN 1978K in the range 4400–7100 Å obtained in 1992 October, 2.7 yr after the latest published spectrum in the Hα region. An

interesting outcome of this observation is the information about the Hα evolution, some new line identifications and a stringent upper limit on the broad Hα flux. We consider in detail an alternative model for the origin of the optical and X-ray emission in SN 1978K. The crucial point of our picture is the interaction of the supernova envelope with dense clumps of the CS wind. The model seems to be successful in reproducing the major optical and X-ray properties of SN 1978K with a moderate mass of CS material.

2 OPTICAL SPECTRUM OF SN 1978K

A CCD spectrum of SN 1978K was obtained on 1992 October 22 with EFOSC2 on the 2.2-m telescope at ESO,

La Silla. Grism #6 combined with a slit width of 1.5 arcsec provided a resolution of approximately 10 Å. The exposure time was 60 min. This spectrum was flux calibrated by observing two standards, EG 21 and LTT 1788, with a slit width of 5 arcsec.

Direct imaging photometry in the *B*, *V*, *R*, *I* bands was obtained with the same instrumentation on 1992 October 22 and with EMMI on the NTT on 1992 October 16.

The resultant spectrum of 1992 October 22 shown in Fig. 1 covers the wavelength range from 4400 to 7150 Å. The list of the spectral lines in Table 1 contains the observed line centres, identifications and fluxes. The corrected line intensities given in the additional column correspond to the total absorption in our and the host galaxy $A_V = 0.64$ mag.
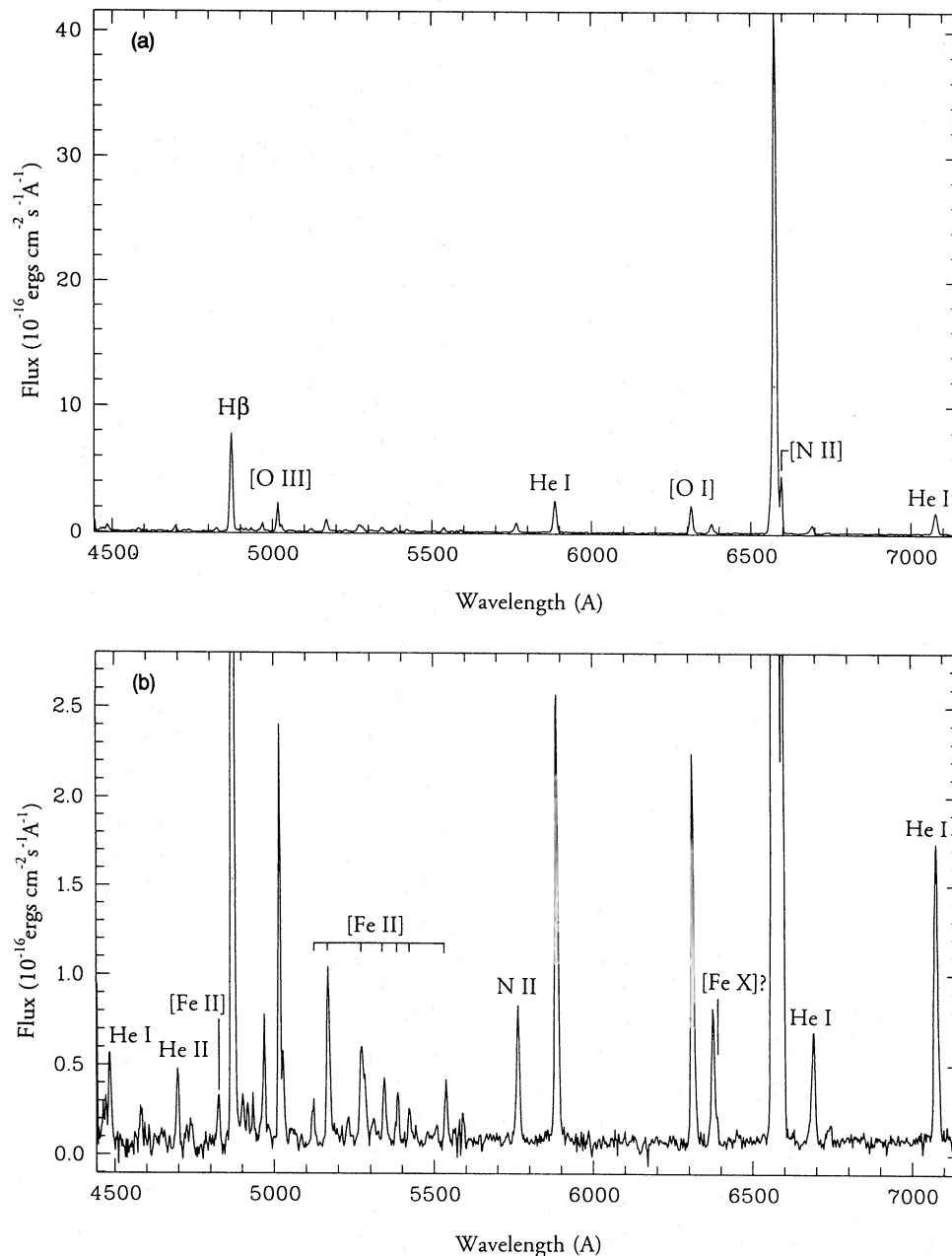

Figure 1. Optical spectrum of SN 1978K of 1992 October 22 obtained with the 2.2-m telescope ESO, La Silla. Full coverage (a) of the flux demonstrates the intensities of the different lines compared with Hα. Expansion of the flux axis (b) shows low-intensity lines.

Table 1. Spectral-line identifications and relative fluxes.

λ Å	Ion	λ_0 Å	F^a $H\alpha = 1000$	F^b $H\alpha = 1000$
4482	He I	4471	9	12
4578	Mg I]	4578	4	5
4693	He II	4686	9	12
4821	[Fe II]	4813	6	8
4868	Hβ	4861	141	180
4965	[O III]	4959	9	11
5013	[O III]	5007	33	41
5023	He I	5015	5	6
5117	[Fe II]	5111	5	6
5165	[Fe II]	5159	19	22
5230	[Fe II]	5220	2.7	3.2
5269	[Fe II]	5262	16	19
5305	[Fe II]	5297	3	5^c
	[Fe XIV]	5303	≤ 1.4	≤ 1.4
5339	[Fe II]	5334	8	9
5381	[Fe II]	5376	4	5
5418	[Fe II]	5413	4	5
5438	[Fe II]	5434	3	3.5
5760	[N II]	5755	16	18
5881	He I	5876	52	56
6307	[O I]	6300	43	44
6370	[O I]	6364	14	14
6382	[Fe X]	6375	1.7	1.7
6569	Hα	6563	1000	1000
6589	[N II]	6584	72	72
6684	He I	6678	15	15
7070	He I	7065	41	39

$^a A_V = 0$, $F(H\alpha) = 5.8 \times 10^{-14}$ erg cm^{-2} s^{-1}.
$^b A_V = 0.64$ mag, $F(H\alpha) = 8.9 \times 10^{-14}$ erg cm^{-2} s^{-1}.
^{c}Possibly blended with [Fe XIV] 5303 Å.

This value has been obtained by Ryder et al. (1993) from 21-cm absorption. The redshift of NGC 1313 is $+254$ km s^{-1} (de Vaucouleurs et al. 1977). We found, however, that the actual mean redshift of spectral lines is 540 ± 50 km s^{-1}, consistent with the redshift 510 km s^{-1} derived by Ryder et al. (1993) for the January 1990 spectrum. The observed Hα width FWHM 560 km s^{-1} is comparable with the width of the instrumental profile, which makes the line profile deconvolution problematic. Therefore only an upper limit of the width FWHM≤ 560 km s^{-1} can be established. In the spectrum of January 1990 Ryder et al. (1993) found for the Hα line a FWHM ≈ 560 km s^{-1}. This value may be adopted for October 1992. It is remarkable that the Hα line in SN 1986J had a similar width (Leibundgut et al. 1991).

The spectrum is dominated by Hα which contains ≈ 60 per cent of the total line luminosity in the optical band. With the absorption $A_V = 0.64$ and the distance of 3.7 Mpc (Tully 1988) the Hα luminosity is 2.2×10^{38} erg s^{-1}, which is 1.5–2 times lower than that resulting from the Hα CCD image and R-band data obtained in 1989 and 1990 by Ryder et al. (1993). The measured value of the Hα from our narrow-slit spectrum should be scaled according to the R-band photometry. All published luminosities have been scaled to an assumed distance of 3.7 Mpc. The Balmer decrement Hα/Hβ is 5.5, i.e. in excess of the recombination nebular case B. In this respect SN 1978K reminds one of SN 1986J, where an even steeper Balmer decrement, 30 in 1986 and 7 in 1989, was found by Leibundgut et al. (1991). Basically, the steep Balmer decrement is an indicator of a large optical depth in the Balmer lines and therefore of the large column density of the partially ionized gas. Apart from strong hydrogen, He I, [O I] and [O III] lines, the spectrum shows a rich set of weaker lines, mostly [Fe II]. The latter are generally characteristic of 'warm' (5000–7000 K) partially ionized gas in the cool zone of a radiative shock wave (SNR and HH-objects).

A matter of special interest is the possible presence of [Fe X] 6374-Å and [Fe XIV] 5303-Å coronal lines, which might originate from a hot ($\sim 10^6$ K) shocked gas. The red wing of the [O I] 6364-Å line shows an additional feature at the position of [Fe X] 6374 Å. The intensity of the [Fe X] line presented in Table 1 was derived using a deblending procedure. Another coronal line, [Fe XIV] 5303 Å, is blended with the [Fe II] 5297-Å line. An upper limit of the flux of the [Fe XIV] line may be found using the intensity ratio of [Fe II] lines 5297 Å and 5376 Å. Both belong to the same multiplet 19F and have a common upper level. The theoretical ratio of intensities 5376 Å/5297 Å is equal to the ratio of spontaneous decay rates, which is 2.8 (Fuhr, Martin & Wiese 1988). The residual (cf. Table 1) may be attributed to the [Fe XIV] line or at least may be considered as an upper limit, if another unidentified line contributes. The coronal [Fe X] line was identified recently in SN 1988Z and its presence is suggested in SN 1986J (Turatto et al. 1993), while the [Fe XIV] line has been detected in supernova remnants (SNRs) (Danziger 1983).

The spectrum does not reveal a broad (3000–10 000 km s^{-1}) Hα emission line which is characteristic of some SN II interacting with a dense CS wind, e.g. SN 1980K and 1979C at the age of ≈ 10 yr. The upper limit of the luminosity of broad Hα from SN 1978K on 1992 October 22 with half-width at zero-intensity (HWZI) ~ 3000–10 000 km s^{-1} is 3×10^{36} erg s^{-1}. For reference the luminosity of broad Hα (HWZI ≈ 6300 km s^{-1}) in SN 1979C at the phase of 11.5 yr is $\approx 7 \times 10^{37}$ erg s^{-1} (Fesen & Matonick 1993), while the luminosity of broad Hα in SN 1980K at age 8 yr is 3×10^{37} erg s^{-1} (Fesen & Becker 1990). If we allow for the possible evolution of the broad Hα luminosity, $L \propto t^{-1}$ (Chevalier & Fransson 1994), we conclude that the luminosity of a broad Hα line in SN 1978K is roughly six times lower compared to that of SN 1980K extrapolated to 14.4 yr, the age of SN 1978K.

The evolution of the Hα luminosity in SN 1978K is traced fairly well by the R magnitude, since Hα is dominant in this band. The R magnitudes from Ryder et al. (1993) converted into Hα luminosities are shown in Fig. 2, together with Hα
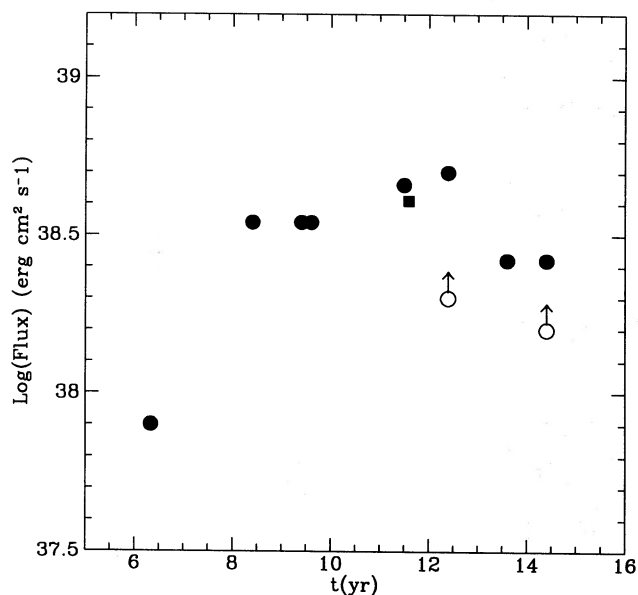
Figure 2. Evolution of the Hα luminosity of SN 1978K. The outburst moment is assumed to be 1978 June 1. Filled dots result from the conversion of R magnitudes into Hα fluxes, where the photometry was compiled by Ryder et al. (1993), except for the last point which comes from the present paper. Contamination by other lines and the continuum in the passband of the R filter should not exceed 10–20 per cent. The filled square results from the above authors' CCD photometry using an Hα filter and corrected by us. The open circles result from the spectrophotometry provided by the above authors and the present paper. Lower limits are suggested because of the small slit sizes used for these observations.

Figure 3. Schematic representation of the interaction of the SN ejecta with a cloud in the CS wind. The SN ejecta drives the cloud shock wave which is a boundary between the pre-shock region A (or leading H II region) and the post-shock hot cooling region B. Soft X-rays emitted by zone B create the leading H II region A, which is responsible for the emission of narrow [O III] lines, and the trailing H II region C, the main source of Hα quanta. The cool partially ionized gas of region D is the site of the emission of [Fe II] and [O I] lines. The dashed line is the reflected shock-wave (bow-shock).

fluxes derived from our more recent R-band photometry and spectroscopy. In spite of the possible systematic errors, the plot of Hα luminosity shows an evident evolution. Between 6.3 and 8.4 yr Hα became stronger by more than a factor of 4, and after a wide maximum between 9 and 13 yr the Hα luminosity began to decrease. In the mechanism of the ejecta-wind interaction this evolution might be understood as an effect of the non-monotonic distribution of the CS material along the radius.

3 THE ORIGIN OF THE OPTICAL EMISSION

3.1 General considerations

The striking similarity between the two late-time supernovae SN 1986J and SN 1978K (strong narrow optical lines, powerful X-ray and radio emissions) suggests that in both cases the same mechanism operates for generating the optical luminosity. Earlier the interaction of the expanding supernova envelope with the cloudy CS wind had been proposed for SN 1986J (Chugai 1993) to account for the low velocity of the optical gas and high velocity of the supernova ejecta as indicated by the high expansion velocity of the radio shell (Rupen, Bartel & Foley 1991). According to this picture the optical emission of SN 1978K at the age of 7–14 yr originates from slow radiative shock waves driven into the numerous dense clouds of the circumstellar wind by the dynamical pressure of the expanding supernova envelope
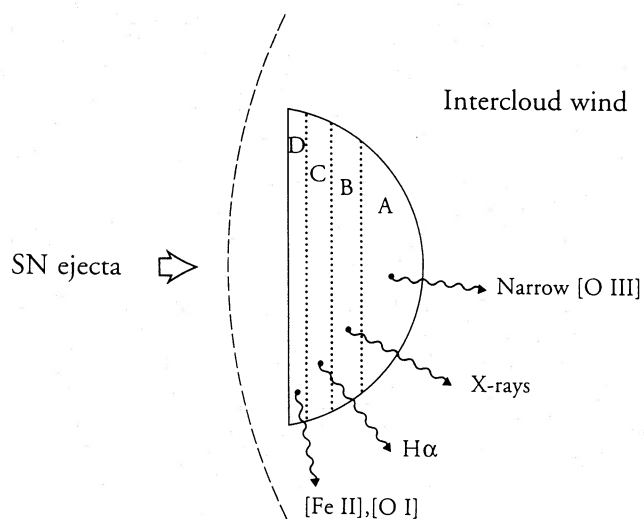
and swept-up intercloud wind. Because of the large density contrast between clouds and ejecta the cloud shock wave is slow enough to account for the low velocity of the line-emitting gas. The width of the Hα profile (FWHM 560 km s^{-1}) is indicative of the radial motion of the emitting gas with the rms velocity ≈ 400 km s^{-1}, which we attribute to the characteristic velocity of the cloud shock waves. The corresponding post-shock equilibrium kinetic temperature is 2.2×10^6 K (≈ 0.2 keV).

One may distinguish (cf. Daltabuit, MacAlpine & Cox 1978) four different zones (Fig. 3) in the shocked cloud: (A) a leading H II region created by the radiative precursor; (B) a post-shock cooling region; (C) a trailing H II region produced by the absorption of XUV radiation from the cooling zone; (D) an H I region. All these zones seem to be represented by emission lines seen in the spectrum of SN 1978K.

Of particular interest is the leading H II region, which must be the site of the narrow lines in contrast to the post-shock zone. Narrow [O III] lines, which are unresolved according to Ryder et al. (1993), may well originate from the undisturbed leading H II region A (Fig. 3). The 4363 Å/5077 Å line ratio indicates a density of 10^{6-7} cm^{-3} (Ryder et al. 1993), which we attribute to the undisturbed cloud density (zone A). The post-shock cooling zone B emits mostly in the EUV and soft X-ray (0.2-keV) band. It may, however, also be a site for the weak coronal [Fe x] and [Fe xiv] lines. The Hα line is emitted by the trailing H II region (zone C), while the neutral hydrogen (zone D) and/or interface between C and D zones is possibly responsible for the emission of the [Fe II] lines and [O I].

The trailing H II region may also contribute to the [O III] flux. Observations indicate, however, that the broad (FWHM

≈ 500 km s^{-1}) component must be weak. The model seems to be consistent with this fact. Actually, computations by Daltabuit et al. (1978) for the case of the radiative shock wave with $u_c = 1000$ km s^{-1} and pre-shock density 10^7 cm^{-3} show that the contribution of the trailing H II region to the [O III] line flux is small, less than 5 per cent of the [O III] emission from the leading H II region.

The interaction of the ejecta with the relatively rarefied intercloud wind proceeds in a standard fashion with the formation of a double shock structure consisting of the outer and inner (or reverse) shock waves in the SN ejecta (cf. Chevalier 1992). In the case of the moderate wind density, $\dot{M} < 10^{-4}$ M$_\odot$ yr^{-1}, both shock waves are adiabatic. The radius R_s and velocity v_s of the intercloud shock wave in SN 1978K can be estimated from the self-similar Chevalier–Nadyozhin solution (Chevalier 1982; Nadyozhin 1985). We describe the density distribution in the supernova envelope by a plateau $\rho = $ constant in the inner part ($v < v_0$) and a power law $\rho \propto v^{-k}$ in the outer layers ($v > v_0$). This law with $k \approx 8$ is a good first approximation of the hydrodynamical models of supernova explosions (see e.g. Chevalier & Fransson 1994). For $k = 8$, according to the self-similar solution, the shock-wave radius evolves then as

$$R_s = \left(\frac{3}{16}\frac{M}{w}\right)^{1/6}(v_0 t)^{5/6}, \qquad v_s = \frac{5}{6}\frac{R_s}{t}. \qquad (1)$$

The value $(3M/16w) = R_{s0}$ is the radius at which the supernova ejecta with velocity $v > v_0$ becomes shocked. The self-similar law (equation 1) evidently is not applicable at times $t > t_{s,0} = R_{s0}/v_0$. Let us estimate the critical time $t_{s,0}$ in the case when a possible counterpart of SN 1978K is SN II-L, which is favoured by the optical photometry in 1978 (cf. Ryder et al. 1993). For the standard value of the kinetic energy $E = 10^{51}$ erg, and ejecta mass 5 M$_\odot$, which is characteristic of SN II-L (Chugai 1990), the kink velocity is $v_0 = 4470$ km s^{-1}. If we assume that the intercloud wind is moderately dense, $w = 2 \times 10^{15}$ g cm^{-1}, comparable with the wind in SN 1980K (cf. Lundqvist & Fransson 1988) we get $t_{s0} = 32$ yr, which means that the self-similar solution is valid. For the same set of parameters the radius of the shock wave at $t = 14.4$ yr according to equation (1) is $R_s = 2.5 \times 10^{17}$ cm, while the velocity $v_s = 4900$ km s^{-1}. The uncertainty of the wind density parameter and mass of ejecta does not affect strongly the derived values, because the dependence on these parameters is very weak, $\propto w^{-1/6}$ and $\propto M^{-1/4}$ (cf. equation 1).

If, however, the mass of the SN 1978K ejecta is very low, e.g. $M \approx 1$ M$_\odot$, as in SN 1988Z (Chugai & Danziger 1994), the Chevalier–Nadyozhin solution for the same wind density parameter $w = 2 \times 10^{15}$ g cm^{-1} becomes invalid already at an early phase, $t > 6$ yr. In this extreme limit the radius of the shock wave can be estimated from the blast wave solution with the finite mass of the ejecta (Chugai & Danziger 1994)

$$\frac{R_s}{R_1} = \left(1 + \frac{t}{t_1}\right)^{2/3} - 1, \qquad (2)$$

where $R_1 = M/w$ and $t_1 = (2R_1/3)(M/E)^{1/2}$. If we adopt $M = 1$ M$_\odot$ we find $R_s = 2.9 \times 10^{17}$ cm at $t = 14.4$ yr, assuming the same w and E. In fact, this radius is slightly overestimated since the solution, equation (2), neglects the initial phase

~ 10 yr of the ejecta deceleration. Therefore the value $R_s = 2.5 \times 10^{17}$ cm obtained above seems to be also appropriate in the latter case.

The turn-on around 1985 ($t \approx 7$ yr) of the R flux, which reflects mainly the behaviour of Hα (Fig. 2), corresponds to the radius $R_s \approx 1.4 \times 10^{17}$ cm in both models of the expansion considered above (cf. equations 1 and 2). The phase of maximum Hα luminosity between 7 and 14 yr presumably corresponds to the interaction of the supernova ejecta with a shell-like distribution of the dense CS wind in the range 10^{17}–3×10^{17} cm. The effects of the ejecta-wind interaction in the inner zone $r < 10^{17}$ cm were not weak, however. Actually, the radio luminosity of SN 1978K at the age of 3 yr (Ryder et al. 1993) was comparable with that of SN 1979C, one of the most powerful radio type-II supernovae.

3.2 Parameters of 'optical' clouds

The velocity of the cloud radiative shock wave driven by the dynamical pressure of the SN ejecta is determined by the pressure equilibrium condition, which may be written in the useful approximate form

$$\rho_c u_c^2 \approx \frac{E}{V}, \qquad (3)$$

where ρ_c is the cloud density, and $V = (4\pi/3)R_s^3$ is the volume occupied by the ejecta and the swept-up wind. The velocity of the radiative shock wave is equal to the velocity of cool post-shock gas. Therefore the typical shock wave velocity responsible for optical lines is $u_c = 400$ km s^{-1}. If we take $E = 10^{51}$ erg and $R_s = 2.5 \times 10^{17}$ cm we obtain in this case $\rho_c = 9.5 \times 10^{-18}$ g cm^{-3} and a hydrogen number density $n_c = 4 \times 10^6$ cm^{-3} (assuming an H abundance of 0.7). It is essential that the derived density is consistent with the requirement that in the [O III] line-emitting region (in our case the leading H II region) the electron density must be 10^{6-7} cm^{-3}.

The lower limit of the cloud radius a is defined by the condition that the shock wave in the cloud is radiative. This means that the dynamical time should exceed the cooling time

$$\frac{a}{u_c} > \frac{\rho_c u_c^2}{32 n_c^2 \Lambda}, \qquad (4)$$

where Λ is a cooling function, while the post-shock density is taken to be four times the pre-shock density. For a post-shock temperature $T_s = 0.2$ keV the cooling function is $\Lambda \approx 10^{-22}$ ergs cm^{-3} s^{-1}. With $n = 4 \times 10^6$ cm^{-3} one obtains a lower limit $a > 2 \times 10^{13}$ cm. If we assume that the cloud sizes are similar to those in clumpy asymptotic giant branch (AGB) winds, we adopt $a \approx 3 \times 10^{15}$ cm, which is equal to the size of H I clouds in the young planetary nebula Helix at radii $\approx 10^{17}$ cm (Meaburn et al. 1992). For the cloud radius 3×10^{15} cm one obtains a mass of cloud 4×10^{-4} M$_\odot$ and the life-time of a shocked cloud $a/u_c \sim 3$ yr.

The Hα flux produced by the reprocessing of the XUV radiation of the cooling region in the cool regions C and D (Fig. 3) may be expressed via the total flux of the kinetic energy in the shock wave, $(\frac{1}{2})\rho_c u_c^3$, and the efficiency ψ of the transformation of this flux into Hα. The estimate for ψ can

be obtained in the approximation that the number of emitted Hα photons in the trailing H II region is equal to half of the ionizing ($E > 1$ Ry) photons produced in the cooling zone. In the case of the exponential spectrum of the radiation emitted by the cooling zone with temperature T_s the efficiency is

$$\psi = \frac{h\nu_{23}}{2kT_s} E_1\left(\frac{\text{Ry}}{kT_s}\right), \tag{5}$$

where ν_{23} is the frequency of an Hα photon and $E_1(x)$ is the first exponential integral. For $T_s = 0.2$ keV one obtains $\psi = 0.01$. The additional ionization produced by photo-electrons in the region of partially ($x \lesssim 0.5$) ionized hydrogen (the interface between C and D zones) doubles this value, resulting in $\psi \approx 0.02$. This means that the observed Hα luminosity of $\approx 2.2 \times 10^{38}$ erg s^{-1} requires an XUV luminosity of shocked clouds of $\approx 10^{40}$ erg s^{-1}.

The number of shocked clouds N_c required to produce the observed luminosity of Hα is determined by the total Hα luminosity

$$L(\text{H}\alpha) = \tfrac{1}{2}\psi\pi a^2 N_c\rho_c u_c^3. \tag{6}$$

For $L(\text{H}\alpha) = 2.2 \times 10^{38}$ erg s^{-1}, $\psi = 0.02$, $a = 3 \times 10^{15}$ cm, $n_c = 4 \times 10^6$ cm^{-3} and $u_c = 400$ km s^{-1} one obtains $N_c = 1300$. The covering factor of these clouds (the relative fraction of sphere subtended by clouds) is 0.05 and the total mass of the shocked clouds is $\approx 0.7\,\text{M}_\odot$. The dynamical lifetime of clouds with the adopted radius is long, ≈ 20 per cent of the age of SN 1978K, which means that a total mass of the swept-up clouds is of the same order of magnitude, i.e. $\sim 1\,\text{M}_\odot$. For reference, the mass of the swept-up intercloud wind is $wr \approx 0.3\,\text{M}_\odot$, if one assumes the density parameter $w = 2 \times 10^{15}$ g cm^{-1}. Thus, the total mass of the CS wind swept-up by the fast shock-wave up to the age 14.4 yr, i.e. in the region $r \lesssim 2.5 \times 10^{17}$ cm, is determined mainly by the cloudy component being of the order of $1\,\text{M}_\odot$. The corresponding average density parameter is $w \approx 10^{16}$ g cm^{-1} while the mass-loss rate is of the order of $\approx 2 \times 10^{-4}\,\text{M}_\odot$ yr^{-1} (for $u_w = 10$ km s^{-1}). In fact the total mass of the CS envelope is probably larger at the expense of the outer, yet unshocked, CS wind.

3.3 Coronal lines

An order-of-magnitude estimate for the expected flux in the [Fe x] and [Fe xiv] coronal lines from cloud shock waves can be obtained from a simple model of the temperature and density evolution in the post-shock region. We will adopt the isobaric condition, constant velocity of post-shock gas relative to the shock-front ($v_s/4$) and constant cooling function $\Lambda = 1.25 \times 10^{-22}$ ergs cm^3 s^{-1}, which is a good approximation in the range 0.4×10^6–2.2×10^6 K. The total flux in the coronal line is determined by the emission measure integral in the range of temperatures of survival of a given ion. In the coronal model the abundance curve FWHM for [Fe xiv] corresponds to the temperature range 1.8×10^6–2.6×10^6 K, while for [Fe x] this range is 0.8×10^6–1.6×10^6 K with an amplitude in both cases of $\phi = 0.25$ (cf. McCray 1987). The resultant ratio of coronal line flux to Hα may be written in the form

$$\frac{F}{F(\text{H}\alpha)} = \phi Q \frac{n_{\text{Fe}}}{n_{\text{H}}} \frac{qh\nu}{\psi\Lambda}. \tag{7}$$

Here Q is the factor determined by the emission measure integral and equals 0.8 and 0.2 for [Fe x] and [Fe xiv], respectively. If we use collisional excitation coefficients for coronal lines q from Blaha (1969), and substitute the relevant values, we obtain for a solar abundance the predicted ratio 0.0036 for [Fe x] 6374 Å/Hα and 0.002 for [Fe xiv] 5303 Å/Hα. The former is only a factor of 2 larger than the observed one (see Table 1), while for [Fe xiv] the prediction is 1.4 times larger than the observational upper limit, which we consider satisfactory, bearing in mind the simplified model used.

4 X-RAY-EMITTING GAS

The X-ray flux from SN 1978K observed by *ROSAT* has been interpreted (Ryder et al. 1993) as thermal radiation with the exponential spectrum $kT = 0.5$ keV (shock-wave velocity $u_x = 630$ km s^{-1}), absorption column density 4×10^{21} cm^{-2} and unabsorbed luminosity $L_x = 6.4 \times 10^{39}$ ergs s^{-1}. The shock-wave velocity required to reproduce an X-ray temperature is 1.6 times larger than the velocity of optical line-emitting gas. It should be emphasized that the soft X-rays with $kT = 0.2$ keV from the 'optical' clouds with the column density $\sim 10^{22}$ cm^{-2} are severely absorbed by the cloud gas, so that the soft component does not contribute noticeably to the observed X-ray flux. (We are indebted to Silvia Pellegrini for checking the possibility of the presence of a soft X-ray component in *ROSAT* data.)

The pre-shock density of the X-ray clouds estimated from pressure equilibrium (equation 2) is $\rho_x \approx 3.9 \times 10^{-18}$ g cm^{-3} and the hydrogen number density is $\approx 1.6 \times 10^6$ cm^{-3}, which is ≈ 0.4 times the density of optical clouds. The emission measure of the X-ray-emitting plasma is $\approx 5 \times 10^{62}$ cm^{-3}. When combined with the density this leads to the mass of the X-ray-emitting plasma as $\approx 0.1\,\text{M}_\odot$. If the post-shock column density is of the order of the cooling column density ($\approx 10^{21}$ cm^{-2}) then the covering factor for X-ray clouds is

$$C_x = L_x(2\pi r_s^2\rho_x u_x^3)^{-1} \approx 0.03. \tag{8}$$

The straightforward conjecture explaining the difference between the parameters of X-ray and optical gas is a model of two populations of wind clouds consisting of 'X-ray' clouds and more dense 'optical' ones. This model has been exploited in the case of SN 1986J (Chugai 1993). On the other hand, the difference between the parameters of the X-ray and optical gas is surprisingly small: the density and covering factor of 'X-ray clouds' are only a factor of 2 lower compared to those of 'optical clouds'. Therefore it is tempting to suggest that a single population of clouds is responsible for both the optical and X-ray emission of SN 1978K. For example, one might imagine that clouds have an inhomogeneous structure: a dense core and a rarefied boundary layer. Then the observed 0.5-keV X-rays may be identified with the relatively fast shock wave propagating in the boundary layer, while the optical emission may be related to the shock wave propagating in the cloud core. The absorption of X-ray radiation could be produced on the spot by the cloud itself, which has a radial column density of the order of 10^{22} cm^{-2}. Unfortunately the poorly known properties of the cloud boundary layer do not allow further quantitative development of the model of a single cloud population.

The shock wave in the boundary layer responsible for the observed X-rays is radiative, which raises a question about

the possible presence of broader optical lines (HWZI 630 km s^{-1}) from the cool recombined gas of the boundary shock wave. The observed profiles do not rule out the presence of such a component. On the other hand, the dense, cool post-shock gas in the boundary layer may be subjected to fragmentation via the Kelvin–Helmholz instability with a subsequent entrainment by the fast flow. This would result in the weakening of the broader optical component.

5   DISCUSSION AND CONCLUSION

The model of the interaction of the expanding supernova envelope with the clumpy CS wind seems to account for the basic properties of the phenomenon of SN 1978K in the optical and X-ray regions at an age ~ 10–14 yr. The mass of CS material involved in the dynamical interaction at this moment is moderate, $\approx 1\,M_\odot$, which corresponds to the mass-loss rate of the pre-supernova of the order of $2\times 10^{-4}\,M_\odot\,\mathrm{yr}^{-1}$ ($u_w = 10$ km s^{-1}). Ryder et al. (1993) also postulate the shock-wave mechanism for the optical emission, but assume a large amount of CS material ($>80\,M_\odot$), which is in fact superfluous. Compared to the model by Ryder et al. (1993) we use a pre-shock density 20 times higher, a shock-wave velocity 2 times higher (400 km s^{-1} instead of 200 km s^{-1}), and an efficiency of the Hα emission 3 times higher.

The evolution of the Hα luminosity (Fig. 2) suggests a variation of the wind density and/or clumpiness along the radius which may represent the shell-like structure of the dense CS clumpy material between 10^{17} and 3×10^{17} cm. With the wind velocity 10 km s^{-1} these radii correspond to the period in the mass-loss history of the pre-supernova 3×10^3–10^4 yr prior to the explosion. Yet it should be noted that SN 1986J between 4 and 9 yr shows a monotonic decline of Hα flux (Leibundgut et al. 1991), thus indicating the absence of the shell-like structure of the CS wind at similar radii.

So far we know only one close analogue of SN 1978K, namely, SN 1986J. Their common properties at the age ~ 10 yr are: strong narrow (FWHM 500–600 km s^{-1}) Hα with the luminosity (several)$\times 10^{38}$ erg s^{-1}; powerful X-ray emission $L_x \sim 10^{40}$ erg s^{-1}; strong radio emission L_ν(6 cm) $\sim 10^{27}$ and 10^{28} erg cm^{-2} s^{-1} Hz^{-1}, for SN 1978K and SN 1986J, respectively. The interaction of the ejecta with a clumpy wind seems to be operating in both cases and the mass-loss rate determined by the clumpy component is of the same order of magnitude, $\approx 10^{-4}\,M_\odot\,\mathrm{yr}^{-1}$.

The fast supernova ejecta is the principal constituent of the ejecta–wind interaction mechanism in both objects. In SN 1986J the existence of the high-velocity ejecta follows from the radio-shell expansion (Rupen et al. 1991). In the case of SN 1978K, however, we have as yet no direct evidence for the presence of the fast ejecta. VLBI measurements with an angular resolution of 0.005 arcsec might detect a fast-expanding radio shell of SN 1978K.

Another way to reveal the fast ejecta is to detect the broad emission lines. The unshocked supernova ejecta ionized by X-rays from the shock waves re-emits absorbed energy in the broad emission lines (Fransson 1984). This mechanism explains the broad emission lines in SN 1980K at an age of 2–9 yr (Chugai 1988, 1992) and in SN 1979C at 11–12 yr (Chevalier & Fransson 1994). In SN 1978K the luminosity of the broad Hα line from ejecta is at least six times lower

compared to SN 1980K (cf. Section 2). In SN 1986J also there is no clear evidence of the broad component (Leibundgut et al. 1991). This paradox may be resolved if one suggests that the ejecta is of low mass and therefore of low emission measure. For a supernova envelope with a mass $M \lesssim 2\,M_\odot$ the expected Hα luminosity will be less than the observed upper limit 2×10^{36} erg s^{-1} in SN 1978K. It is remarkable that the low mass of the ejecta ($\sim 1\,M_\odot$) has been derived from different considerations in the case of SN 1988Z, another SN II with a dense clumpy CS wind (Chugai & Danziger 1994). Another factor for suppressing Hα luminosity is the possible underabundance of hydrogen in the supernova envelope.

The optical response of the unshocked ejecta in broad emission lines is a powerful diagnostic tool for supernovae, the nature of which is still vague and capricious. Therefore it would be highly desirable to observe both supernovae with the resolution ≈ 1000 km s^{-1} and high signal-to-noise ratio to detect any faint broad emission-line components of Hα, He I 5876 Å, and possibly of [O I] and [O III] lines.

REFERENCES

Blaha M., 1969, A&A, 1, 42
Bregman J. N., Pildis, R. A., 1992, ApJ, 398, L107
Chevalier R. A., 1982, ApJ, 258, 790
Chevalier R. A., Fransson C., 1994, ApJ, 420, 268
Chugai N. N., 1988, Ap&SS, 146, 375
Chugai N. N., 1990, SvA Lett., 16, 457
Chugai N. N., 1992, SvA, 36, 63
Chugai N. N., 1993, ApJ, 414, L101
Chugai N. N., Danziger I. J., 1994, MNRAS, 268, 173
Daltabuit E., MacAlpine G. M., Cox D. P., 1978, ApJ, 219, 372
Danziger I. J., 1983, in Danziger I. J., Gorenstein P., eds, Supernova Remnants and their X-ray Emission. Reidel, Dordrecht, p. 193
de Vaucouleurs G., de Vaucouleurs A., Corwin H. G., 1977, Reference Catalogue of Bright Galaxies. 2nd Ed. Austin: Univ. of Texas Press
Fesen R. A., Becker R. H., 1990, ApJ, 351, 437
Fesen R. A., Matonick D. M., 1993, ApJ, 407, 110
Filippenko A. V., 1992, IAU Circ. 5630
Fransson C., 1984, A&A, 133, 264
Fuhr J. R., Martin G. A., Wiese W. L., 1988, J. Phys. Chem. Ref. Data Suppl., 4, 108
Leibundgut B., Kirshner R. P., Pinto P. A., Ruppen M. P., Smith R. C., Gunn J. E., Schneider D. P., 1991, ApJ, 372, 531
Lundqvist P., Fransson C., 1988, A&A, 192, 221
McCray R. A., 1987, in Dalgarno A., Layzer D., eds, Spectroscopy of Astrophysical Plasma. Cambridge Univ. Press, Cambridge, p. 255
Meaburn J., Walsh J. R., Clegg R. E. S., Walton N. A., Tailor D., Berry D. C., 1992, MNRAS, 155, 177
Nadyozhin D. K., 1985, Ap&SS, 112, 225
Rupen M. P., Bartel N., Foley A. R., 1991, in Danziger I. J., Kjär K., eds, SN 1987A and other Supernovae. ESO, Garching, p. 645
Ryder S., Dopita M., 1990, IAU Circ. 4950
Ryder S., Staveley-Smith L., Dopita M., Petre R., Colbert E., Malin D., Schlegel E., 1993, ApJ, 416, 167
Tully B., 1988, Nearby Galaxies Catalog. Cambridge Univ. Press, Cambridge
Turatto M., Cappellaro E., Danziger I. J., Benetti S., Gouiffes C., Della Valle M., 1993, MNRAS, 262, 128
Weiler K. W., Panagia N., Sramek R. A., 1990, ApJ, 364, 611